



Porewater chemistry of Louisiana marshes with contrasting salinities and its implications for coastal acidification

Songjie He ^{a,*}, Kanchan Maiti ^a, Christopher M. Swarzenski ^b, Tracy Elsey-Quirk ^a, Gina N. Groseclose ^a, Dubravko Justic ^a

^a Department of Oceanography and Coastal Sciences, Louisiana State University, Baton Rouge, LA, USA

^b U.S. Geological Survey, Lower Mississippi-Gulf Water Science Center, Baton Rouge, LA, USA



ARTICLE INFO

Keywords:

Porewater
Dissolved inorganic carbon
Alkalinity
Acidification
Coastal marsh

ABSTRACT

Dissolved inorganic carbon (DIC) and total alkalinity (TA) are fundamental components of carbonate systems that control pH and buffering capacity of a water body. Three coastal marshes with contrasting salinities in Barataria Basin, Louisiana, USA, were sampled five times between December 2018 and October 2019 to understand seasonal changes in porewater carbonate chemistry and its impact on surrounding water bodies. Porewater DIC and TA increased with depth irrespective of marsh type and ranged from 4.47 to 31.61 mmol/kg and from 1.78 to 28.56 mmol/kg, respectively. The salt marsh had higher porewater DIC and TA compared to the lower salinity intermediate and brackish marshes, probably due to sulfate reduction in the salt marsh. However, it is likely that denitrification is also an important anaerobic respiration pathway in these marshes because of high nitrate concentrations in this region and low porewater TA/DIC ratios in all three marshes. Porewater TA and DIC concentrations were generally higher during warmer months than colder months. However, the marsh flooding regime had a profound influence on TA and DIC concentrations by changing the redox potential of the marsh soil. Porewater TA/DIC ratios in all three marshes were generally less than 1, while surface water TA/DIC ratios were around 1, suggesting that export of DIC and TA from coastal marshes has the potential to contribute to coastal acidification.

1. Introduction

Marsh carbon dynamics have been the focus of extensive research because of the high rates of carbon fixation by the primary producers and subsequent support of estuarine food webs (Herke et al., 1995; Elsey-Quirk et al., 2011; Baker et al., 2020). The high rate of carbon burial and storage in the wetland soils contributes disproportionately to the global carbon budget relative to their size (Bauer et al., 2013). Marshes are a significant sink for atmospheric carbon dioxide (CO₂), with a net uptake of approximately 5–87 Tg C yr⁻¹ globally and an average carbon burial rate of approximately 218 g C m⁻² yr⁻¹ (Chmura et al., 2003; Duarte et al., 2005; McLeod et al., 2011). Coastal marshes thus represent one of the largest carbon pools in the coastal zone (Chmura et al., 2003). The remineralization of a portion of this large soil organic matter pool and their subsequent exchange with surrounding water bodies can greatly influence the water chemistry of adjacent tidal channels and estuaries.

Marsh porewater tends to have a higher partial pressure of CO₂ (pCO₂), higher concentrations of dissolved inorganic carbon (DIC), and greater total alkalinity (TA) than surrounding surface waters, due to high anaerobic activity in marsh sediments (Wang et al., 2016; Najjar et al., 2018). Alkalinity and DIC production are driven primarily by organic matter decomposition involving a series of redox reactions (Krumins et al., 2013; Sippo et al., 2016, Table 1). In most sediments, organic matter decomposition follows a diagenetic reaction sequence, whereby surface aerobic processes (oxygen as the electron accepter) are followed by anoxic processes (electron accepters are nitrate, manganese, iron, and sulfate), in deeper sediment (Burdige, 2011; Hu and Cai, 2011; Fig. S1). The different microbial respiration processes in soil produce different amounts of DIC and TA for every mole of organic matter respired (assuming Redfield stoichiometry), as shown in Table 1. The concentrations and ratios of TA to DIC resulting from these microbial respiration processes control the pH of marsh porewater. Hydrological processes, such as tidal pumping and groundwater discharge, drive the

* Corresponding author.

E-mail addresses: she5@lsu.edu (S. He), kmaiti@lsu.edu (K. Maiti), cswarzen@usgs.gov (C.M. Swarzenski), tquirk@lsu.edu (T. Elsey-Quirk), ggrose1@lsu.edu (G.N. Groseclose), djusti1@lsu.edu (D. Justic).

Table 1

Major biogeochemical process governing DIC and TA changes in coastal environments (adapted from Krumins et al., 2013 and Sippo et al., 2016).

Reaction Name	Reaction Equation	ΔDIC	ΔTA
Hydrolysis	$(\text{CH}_2\text{O})_{106}(\text{NH}_3)_{16}(\text{H}_3\text{PO}_4) + 15\text{H}^+ \rightarrow 106\text{CH}_2\text{O} + 16\text{NH}_4^+ + \text{H}_2\text{PO}_4^-$	0	+0.14
Aerobic respiration	$\text{CH}_2\text{O} + \text{O}_2 \rightarrow \text{CO}_2 + \text{H}_2\text{O}$	+1	0
Denitrification	$\text{CH}_2\text{O} + 0.8\text{NO}_3^- + 0.8\text{H}^+ \rightarrow \text{CO}_2 + 0.4\text{N}_2 + 1.4\text{H}_2\text{O}$	+1	+0.8
Manganese reduction	$\text{CH}_2\text{O} + 2\text{MnO}_2 + 4\text{H}^+ \rightarrow \text{CO}_2 + 2\text{Mn}^{2+} + 3\text{H}_2\text{O}$	+1	+4
Iron reduction	$\text{CH}_2\text{O} + 4\text{Fe}(\text{OH})_3 + 8\text{H}^+ \rightarrow \text{CO}_2 + 4\text{Fe}^{2+} + 11\text{H}_2\text{O}$	+1	+8
Sulfate reduction	$\text{CH}_2\text{O} + 0.5\text{SO}_4^{2-} + 0.5\text{H}^+ \rightarrow \text{CO}_2 + 0.5\text{HS}^- + \text{H}_2\text{O}$	+1	+1
Methane fermentation	$\text{CH}_2\text{O} \rightarrow 0.5\text{CO}_2 + 0.5\text{CH}_4$	+0.5	0
Primary production	$106\text{CO}_2 + 16\text{NO}_3^- + \text{H}_3\text{PO}_4 \rightarrow (\text{CH}_2\text{O})_{106}(\text{NH}_3)_{16}(\text{H}_3\text{PO}_4)$	-1	+0.2
Carbonate dissolution	$\text{CaCO}_3 \rightarrow \text{Ca}^{2+} + \text{CO}_3^{2-}$	+1	+2
Nitrification	$\text{NH}_4^+ + 2\text{O}_2 \rightarrow \text{NO}_3^- + \text{H}_2\text{O} + 2\text{H}^+$	0	-1
Iron oxidation	$4\text{Fe}^{2+} + \text{O}_2 \rightarrow 4\text{Fe}(\text{OH})_3 + 8\text{H}^+$	0	-8
Sulfide oxidation	$\text{HS}^- + 2\text{O}_2 \rightarrow \text{SO}_4^{2-} + \text{H}^+$	0	-1
Carbonate precipitation	$\text{Ca}^{2+} + \text{CO}_3^{2-} \rightarrow \text{CaCO}_3$	-1	-2

exchange between TA and DIC enriched porewaters and adjacent water bodies (Wang and Cai, 2004; Wang et al., 2016; Najjar et al., 2018). Depending on prevailing conditions, some of the TA and DIC are released to the atmosphere as CO_2 or laterally exported to the coastal ocean, thereby contributing to both carbon export from marshes and buffering or acidification of coastal waters (Raymond et al., 2000; Wang and Cai, 2004; Wang et al., 2016).

Tidal marshes are thus an important source of inorganic carbon to the coastal ocean and play an important role in modulating the buffering capacity of coastal waters (Wang et al., 2016). There have been few studies that quantify inorganic carbon fluxes from marshes or marsh-dominated estuaries into coastal oceans, but it still remains the least measured term in the ecosystem carbon budget (Wang and Cai, 2004; Cai, 2011; Bauer et al., 2013; Wang et al., 2016). DIC export from a marsh-dominated estuary in the southeast USA to adjacent coastal waters has been estimated to be 109 g C m^{-2} (of water) yr^{-1} (Wang and Cai, 2004). In a recent study, loss of inorganic carbon was estimated to be 91% of tidal carbon export in a brackish marsh and may be the most important term limiting C sequestration (Bogard et al., 2020). While these flux estimates provide valuable information on the coastal carbon budget, there are large uncertainties and variabilities in these estimates due to low frequency sampling and scaling (Downing et al., 2009; Ganju et al., 2012; Wang et al., 2016). Using one salt marsh in the northeast USA, Wang et al. (2016) scaled up and calculated DIC export from marshes to the USA East Coast to be $414 \text{ g C m}^{-2} \text{ yr}^{-1}$. Najjar et al. (2018) provided more constrained carbon exchange budgets of wetlands, estuaries, and shelf for US east coast but also included limited studies. The tidal exchange of porewater DIC produced by organic matter respiration in the marsh soil represents a large portion of the exported DIC. However, the exchange of porewater between marshes and adjacent water bodies and the exact contribution of marshes to the net export of DIC is currently poorly understood at both regional and global scales. A robust estimate of marsh DIC export requires measurements in tidal channels as well as in porewater but very few studies included porewater endmembers (e.g., Wang et al., 2016; Guimond et al., 2020; Santos et al., 2021). Therefore, a better understanding of porewater DIC and TA in marsh soils could improve our knowledge of the coastal carbon budget and its impact on possible coastal acidification.

The coastal marshes in the Mississippi River Deltaic region have been undergoing rapid erosion caused by eustatic sea level rise, high

subsidence rates, oil and gas activities, low sediment supply, and infrequent storm events (Snadden et al., 2007; Kolker et al., 2011; Robert and John, 2011; Couvillon et al., 2017; Turner and McClenachan, 2018). Analyses show that coastal Louisiana has experienced a net land loss of approximately 4833 square kilometers from 1932 to 2016, which amounts to a decrease of approximately 25 percent of the 1932 land area (Couvillon et al., 2017). Marsh loss can be expected to release high DIC but low pH porewater to adjacent estuaries due to the increased hydrological exchange (Kindinger et al., 2013) and respiration of the eroded labile carbon (Hayes et al., 2021), which could potentially drive pH variability and contribute to coastal acidification (Ekstrom et al., 2015; Still and Stolt, 2015). In coastal Louisiana, in addition to the widespread rapid conversion of marsh to open water, the boundaries between salt marshes and fresher marshes have been shifting (Couvillon et al., 2017; Linscombe and Hartley, 2011). Marsh type changes could influence the DIC to TA ratio in porewater, which in turn can change the pH of porewater and the surrounding surface water. Further, numerous restoration projects to combat marsh loss are underway, and include river diversions, which will introduce water and sediment from the Mississippi River to flow into deteriorating marsh basins (CPRA, 2017). The proposed Mid-Barataria Sediment Diversion will divert up to $2100 \text{ m}^3/\text{s}$ of fresh water from the Mississippi River directly into the Barataria Basin (CPRA, 2017), which could potentially freshen salt and brackish marshes in its flow path. This influx of colder, nutrient-rich river water will not only change the salinity, but also change marsh soil temperature, flooding regime, and redox potential (Das et al., 2012; Peyronnin et al., 2017; White et al., 2019). Such changes will influence soil respiration processes and porewater exchange (Roberts and Doty, 2015; Shen et al., 2015), which in turn will determine TA and DIC flux between marshes and surrounding water bodies. Such a change could reverse the DIC to TA ratio in porewater by shifting the remineralization pathway of organic matter in the sediment. For instance, the influx of fresh, nutrient-rich Mississippi River water may increase denitrification rate in a salt marsh soil, where sulfate reduction may otherwise be the dominant anaerobic decomposition process.

It is thus important to understand the dynamics of DIC and TA in marsh soils with contrasting salinities to determine how dissolved inorganic carbon dynamics may change in future and impact adjacent water bodies. Since the biogeochemical processes that control DIC and TA are dependent on temperature and redox potential, we conducted our study during different seasons and at different marsh soil depths. We hypothesized that TA/DIC ratio in marsh soils will be higher during summer months due to higher anaerobic respiration in soil, which usually generates more TA than DIC. The exchange of such porewater will result in buffering of adjacent channel waters. To test this hypothesis, we measured seasonal variability in porewater DIC and TA in three contrasting marshes as well as DIC and TA in adjacent channels and creeks.

2. Method

2.1. Study area

The study area is in Barataria Basin, Louisiana, USA, located in the north-central Gulf of Mexico, just to the west of the Mississippi River (Fig. 1). The Barataria estuary is about 120 km long and on average about 2 m deep. The northern half of the estuary contains several large lakes. The southern half of the estuary contains tidally influenced marshes interconnected by ponds, lakes, and channels that finally empty into a large bay system behind barrier islands. Four tidal passes (Barataria, Caminada, Abel and Quatre Bayou) connect the estuary and the Gulf of Mexico. The diurnal tide range in the Barataria Basin is approximately 0.35 m at the coast but decreases by an order of magnitude as the tide progresses inland. Salinities range from near zero in the upper reaches of the estuary to about 25 in the southernmost section of the estuary. Fresh water enters the Barataria estuary mainly from four

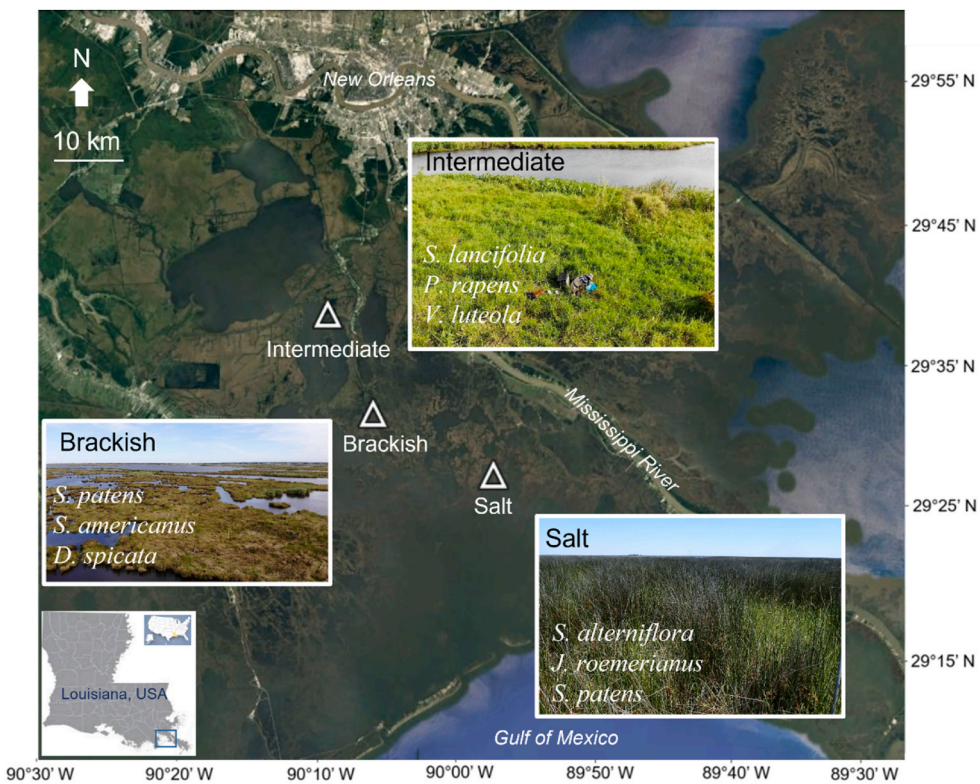


Fig. 1. Three study sites with contrasting salinity in Barataria Basin in Louisiana, USA. The three most abundant plant species are listed for each marsh. Base map is provided by Google Earth.

sources: rainfall, stream runoff, the Mississippi River, and the Gulf Intracoastal Waterway (Das et al., 2012). The region can be characterized as subtropical with long, hot, and humid summers and generally short, mild winters. The average monthly temperature ranged from 12.5 °C in January 2019 to 29.4 °C in August 2019, with a mean of 22.7 °C for the 11-month study period (December 2018 to October 2019). The monthly precipitation totals ranged from 4.8 mm in September 2019 to 316.7 mm in October 2019, with a monthly mean of 149.5 mm for the 11 months (NOAA National Centers for Environmental Information site: New Orleans Airport, LA, USA).

Three marsh types in the Barataria Basin were selected for this study: an intermediate marsh, a brackish marsh, and a salt marsh (Table 2 and Fig. 1). The sites were selected due to their proximity to Louisiana's

Coastwide Reference Monitoring System (CRMS) sites where data on vegetation, hydrology, accretion, elevation change, and land/water composition have been collected for the last 10 years.

2.2. Sample collection

Samples were collected during five field trips at each of the three marshes. The intermediate and brackish marshes were visited on the same day, while separate field trips during the same season were made to the salt marsh (Table 2 and Fig. 1). During each trip, water quality parameters, such as temperature, salinity, specific conductance, dissolved oxygen (DO) concentration were measured in-situ using a YSI handheld meter (YSI professional plus; Yellow Springs, OH). pH was

Table 2

Site characteristics of the three marshes investigated during this study. Soil moisture content, bulk density (BD) and organic matter content (OM) represent the average for the top 24 cm marsh soil. The air temperature and precipitation data are available at NOAA NCEI (National Centers for Environmental Information).

Site	Latitude	Longitude	CRMS				Sampling Date	Air Temp. (°C)	Precipitation for 7 days prior to sampling (mm)	Flooding (visual)
			ID	Moisture (%)	BD (g/cm ³)	OM (%)				
Intermediate	29.6703	-90.1336	4245	83	0.15	38.2	01/08/19	18.1	33.3	No
							03/15/19	18.1	12.2	No
							06/12/19	27.3	16.3	No
							08/21/19	28.3	1.1	No
							10/22/19	22.2	28.0	No
Brackish	29.5598	-90.0733	0220	80	0.17	38.9	01/08/19	18.1	33.3	No
							03/15/19	18.1	12.2	No
							06/12/19	27.3	16.3	Yes
							08/21/19	28.3	1.1	Yes
							10/22/19	22.2	28.0	Yes
Salt	29.4923	-89.9125	0224	77	0.22	31.0	12/18/18	11.9	9.7	No
							02/13/19	12.8	34.8	Yes
							05/15/19	24.5	144.3	Yes
							09/06/19	30.1	0	Yes
							10/28/19	18.6	186.2	Yes

measured using the YSI meter until March 2019, after which a pH meter (Thermo Scientific Orion 2 STAR; Waltham, MA) was used. pH was also calculated (denoted by calculated pH) using measurements of TA, DIC, temperature, pressure, salinity, and the CO2SYS.XLS application (Pierrot and Wallace, 2006), by selecting K_1 and K_2 carbonic acid dissociation constants of Millero et al. (2006), and K_{SO_4} as determined by Dickson (1990).

Porewater samples were collected at both the edge (~1 m from creek) and interior (~30 m from creek) of the marshes for analyses of DIC and TA at 10, 25, and 80 cm below the marsh surface with a syringe attached to a specially designed porewater sampler (Fig. S2). The samplers were made of 90 cm-long clear acrylic rigid tubes with 2.5 mm internal diameter and a luer-lock attachment at one end. The bottom 2 cm of the other end was sealed with epoxy, and 10 holes with diameter of ~1.5 mm were drilled above the bottom seal to allow porewater to seep into the tubes (McKee et al., 1988). The porewater samples were collected after discarding the dead volume inside the sampler (~6 mL) and rinsing the syringe with porewater. Water samples from marsh surface, creeks, and channels were collected directly using a syringe

connected to a tube. For both DIC and TA samples, water samples were passed through a 0.45 mm glass fiber syringe filter and collected without headspace into air-tight 40 mL glass vials, by filling from the bottom and allowing overflow of at least the volume of the vial to minimize atmospheric contamination (Anderson et al., 2020). DIC and TA samples were preserved with 20 μ L saturated mercuric chloride ($HgCl_2$) solution. Water samples were transported to the laboratory on ice and stored at 5 °C until analysis.

Marsh surface water samples were collected if the marsh was flooded during the field trip. Flooding conditions of the three marshes determined by visually inspecting the sampling area during the field trip were not consistent during the field trips (Table 2). For instance, the intermediate marsh surface was never flooded during the five field trips, while the brackish marsh was flooded during three trips and the salt marsh was flooded during all trips except the one in December. The observed flooding conditions at each site were not consistent with the water level data recorded by Louisiana Coastwide Reference Monitoring System (CRMS) (Fig. 2). We attribute this inconsistency to spatiotemporal heterogeneity between the CRMS sites and the sampling sites, even

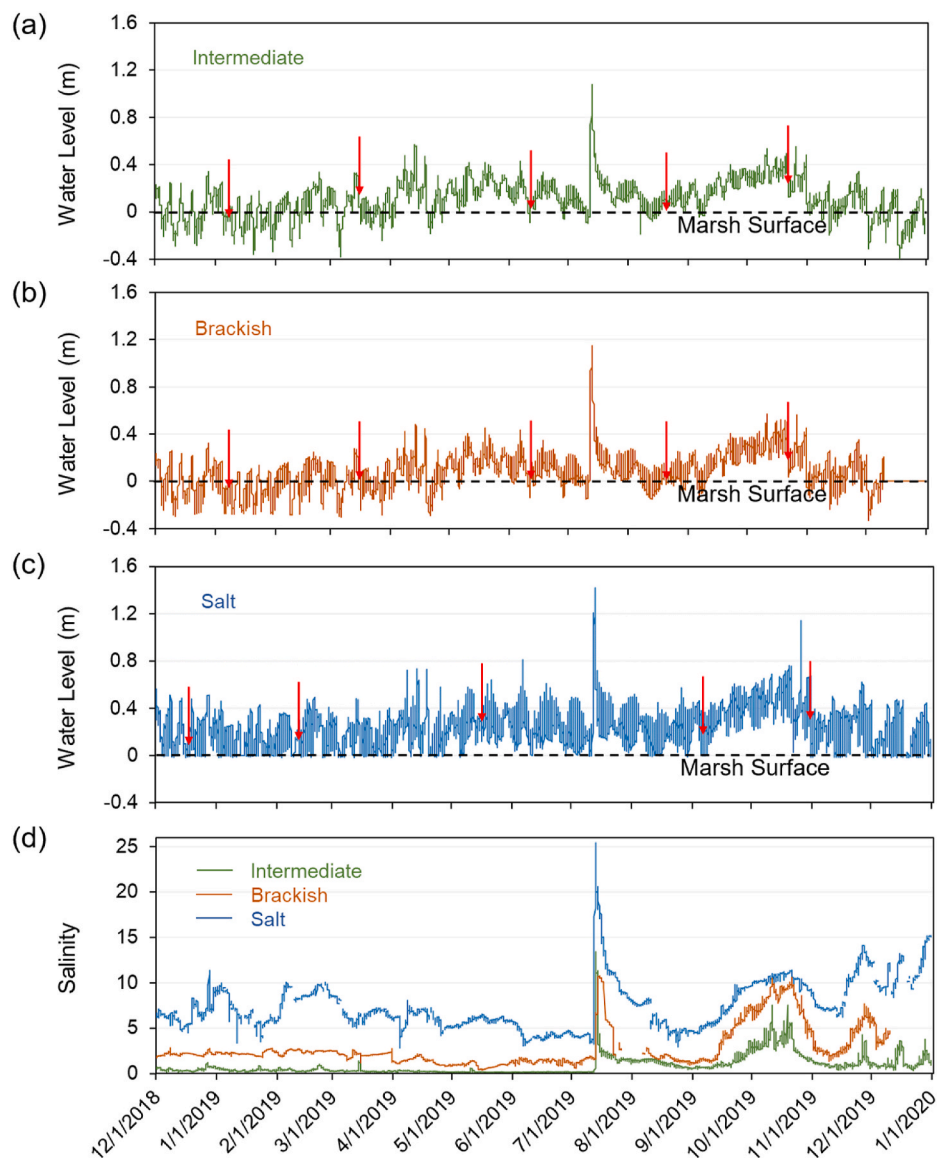


Fig. 2. Surface water level (a, b, c) and salinity (d) of the three marshes. All data used in this figure were collected from near-by CRMS sites. Sampling dates are marked with red arrows. Note that the salt marsh had different sampling dates from the other two marshes. (For interpretation of the references to color in this figure legend, the reader is referred to the Web version of this article.)

though they were in proximity. The observed flooding condition during field trips can be considered site-specific information. However, the continuous data from CRMS is valuable for understanding the seasonal variability in salinity and water level during our study period and their differences between the three marsh sites.

We were unable to collect porewater samples from all three depths at the marsh edge for the intermediate and brackish marshes during many of the trips when the marsh was dry, so there were no porewater to collect at shallower depths. Thus, for comparison between the marshes, only interior porewater data were used and comparison of porewater between marsh edge and marsh interior was only made for the salt marsh site.

2.3. Lab analysis

Dissolved inorganic carbon samples were measured using the standard protocol for the semi-automated system Apollo SciTech AS-C5 Dissolved Inorganic Carbon Analyzer (Newark, DE, USA). Briefly, a 0.5–1 mL sample was acidified by phosphoric acid, and the extracted CO_2 gas was subsequently quantified with a built-in infrared CO_2 detector with a precision $<1\%$ (Cai et al., 1998). Both certified reference material (CRM batch 180; DIC = $2021.87 \pm 0.50 \mu\text{mol/kg}$; Dickson, 2010) and an internal standard of 20.897 mmol/kg NaHCO_3 solution were used to make the standard curves for calculation.

Alkalinity samples were analyzed by Gran titration (Gran, 1952) using the semi-automated system Apollo SciTech AS-ALK2 Total Alkalinity Titrator (Newark, DE, USA). The precision of this method is less than 1% and the analysis were carried out at a controlled temperature of 25°C . The titrator was calibrated using the certified reference material (CRM batch 180; TA = $2224.47 \pm 0.56 \mu\text{mol/kg}$; Dickson, 2010) and a 20.897 mmol/kg NaHCO_3 solution. It is important to note that this alkalinity measurement may include the contribution from organic alkalinity (Cai et al., 1998). A recent study of a salt marsh in the northeast USA found organic alkalinity to contribute 0.9–4.3% of TA (Song et al., 2020).

3. Results

3.1. Soil chemistry

From December 1, 2018 to December 31, 2019, continuous water level data from CRMS showed that the salt marsh was flooded more frequently than the intermediate and brackish marshes (Fig. 2a–c). Seasonally, all marshes were flooded less frequently during the winter and more frequently during the summer and fall. At times of sample collection, the observed flooding conditions differed among marshes. For example, the salt marsh was flooded four out of the five sampling times, while the intermediate marsh was never flooded (Table 2).

Using data collected from CRMS, the average soil moisture content in the upper 24 cm of the intermediate, brackish, and salt marshes was calculated to be 83, 80, and 77%, respectively. All three marshes had similar soil bulk densities and organic matter contents (Table 2). The average dry bulk density of the top 24 cm was 0.15, 0.18, and 0.22 g/cm^3 in the intermediate, brackish, and salt marshes, respectively. The average organic matter content of the top 24 cm was 38.2, 38.9, and 31.0% for the three marshes, respectively, which is similar to the organic content reported in other studies from this region (Ryu et al., 2021a, 2021b). Ryu et al. (2021a, 2021b) also indicated the peat layer to be at a depth $>150 \text{ cm}$, which is deeper than our current sampling depths.

The surface water salinity at surrounding channels/creeks was greater at the salt marsh than at the intermediate and brackish marshes; the differences among the three marshes were most pronounced during the drier winter months (Fig. 2d). Porewater salinities of the three marshes were also different with an increase from the intermediate marsh to the salt marsh (Fig. 3a). The average porewater salinity in the intermediate and brackish marshes was usually less than 5, while the

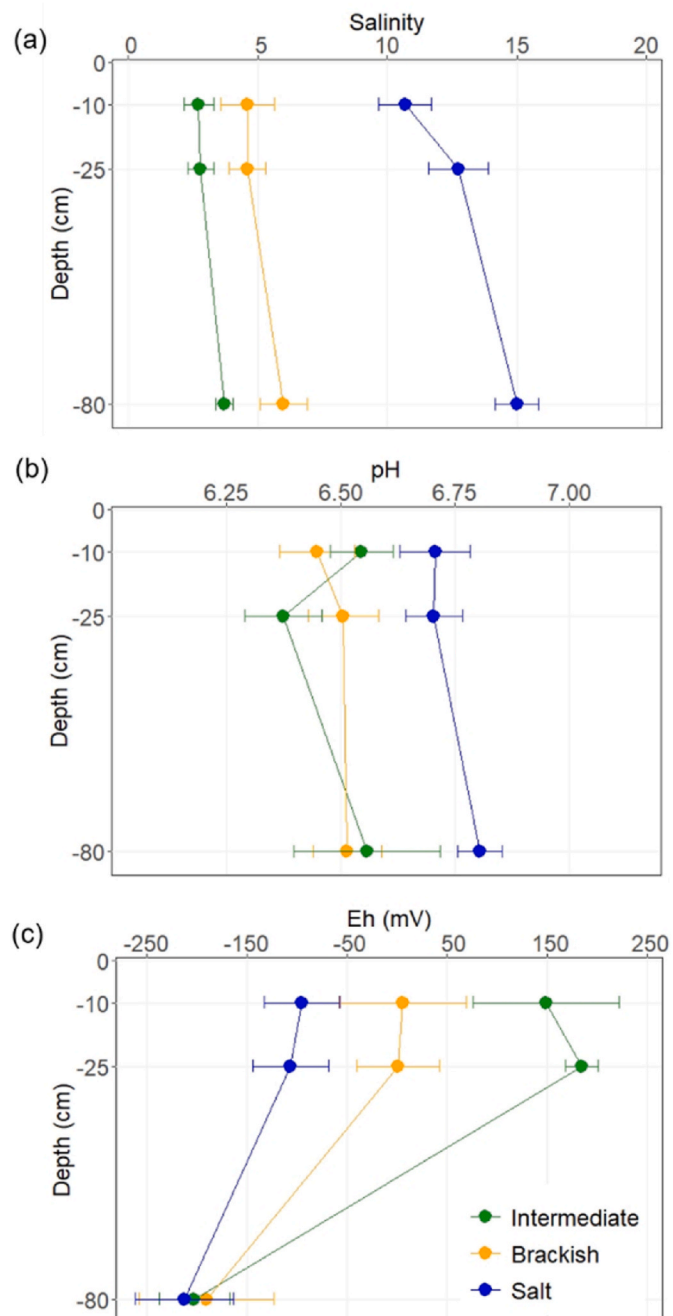


Fig. 3. Porewater (a) salinity, (b) pH, and (c) Eh in the three marshes. Mean values are represented by solid dots, and the horizontal bars represent standard errors. Depth = -10 , -25 , and -80 cm were used to denote porewater sampling depth of 10 , 25 , and 80 cm below the marsh surface. (For interpretation of the references to color in this figure legend, the reader is referred to the Web version of this article.)

average porewater salinity in the salt marsh was generally above 10. In all three marshes, the porewater pH was below 7, with the intermediate and brackish marshes having similar pH, and the salt marsh having a higher pH (Fig. 3b). The redox potential decreased with depth in all marshes with the salt marsh having the lowest redox potential, or most reduced conditions, overall (Fig. 3c).

3.2. Temporal variations of TA, DIC, and TA/DIC ratio

The TA, DIC concentrations and TA/DIC ratios exhibited

considerable variation over time. For instance, the brackish marsh porewater DIC concentration at 10 cm during late summer (August) was 15.50 mmol/kg, which is three times greater than 4.72 mmol/kg recorded in spring (March) (Fig. 4). In general, both TA and DIC concentrations were found to be higher in warmer months than during colder months (Fig. 4). However, for the salt marsh, during the cold but dry season (December), both porewater TA and DIC at 10 and 25 cm were the highest among all five trips. TA/DIC ratios of the intermediate and brackish marshes also were the highest during this season (January). For the salt marsh, porewater TA/DIC ratio was the highest in February.

3.3. Spatial variations of TA, DIC, and TA/DIC ratio

TA was higher in porewater than in the adjacent channels and creeks at all three marshes (Table 3; Figs. 4 and 5). Channel and creek surface water TA concentrations increased from the intermediate marsh to the salt marsh. The intermediate marsh and the brackish marsh had similar porewater TA (Fig. 5a). The average porewater TA concentrations in these two marshes was 8.04 mmol/kg, ranging from 4.52 mmol/kg at the brackish marsh at 10 cm below marsh surface to 13.93 mmol/kg at the intermediate marsh at 80 cm. The salt marsh had higher porewater TA when compared with the other two marshes, ranging from 12.74 to 24.98 mmol/kg (mean = 18.15 mmol/kg). Porewater TA in all three marshes increased with depth, with 80 cm porewater always having the highest TA. Concentrations of DIC were higher than TA concentrations in all three marshes but showed similar patterns as TA (Fig. 4b). The TA/DIC ratios in porewaters of all three marshes were less than 1, except for the salt marsh at 10 cm. The TA/DIC ratio also increased with depth at the intermediate and brackish marshes, but not at the salt marsh.

A comparison of marsh edge and marsh interior TA and DIC concentrations for the salt marsh showed that the marsh interior usually had higher TA and DIC than the marsh edge (Fig. 6). The TA/DIC ratios on the other hand were similar between the marsh edge and interior at 80 cm but differed at 10 cm and 25 cm depths.

Table 3

Mean \pm standard error values for environmental and inorganic carbon parameters in channels and creeks from December 2018 to October 2019. Numbers listed in parentheses are the corresponding sample sizes.

Parameter	Intermediate		Brackish		Salt	
	Channel	Creek	Channel	Creek	Channel	Creek
Salinity	1.22 \pm 0.88 (5)	1.04 \pm 0.55 (5)	2.81 \pm 1.51 (5)	3.07 \pm 1.41 (5)	7.18 \pm 0.88 (6)	7.04 \pm 0.68 (8)
pH	7.78 \pm 0.31 (5)	7.76 \pm 0.39	7.72 \pm 0.43 (5)	7.57 \pm 0.20	7.75 \pm 0.23 (6)	7.53 \pm 0.15 (8)
Calculated pH	7.86 \pm 0.15 (5)	8.04 \pm 0.36	8.24 \pm 0.24 (5)	7.85 \pm 0.28	7.87 \pm 0.18 (6)	7.70 \pm 0.20 (7)
TA (mmol/kg)	1.60 \pm 0.05 (5)	1.59 \pm 0.03	1.74 \pm 0.12 (5)	1.86 \pm 0.09	1.96 \pm 0.08 (6)	2.01 \pm 0.11 (7)
DIC (mmol/kg)	1.63 \pm 0.05 (5)	1.58 \pm 0.06	1.69 \pm 0.12 (5)	1.87 \pm 0.08	1.92 \pm 0.09 (6)	2.03 \pm 0.11 (7)
TA/DIC	0.98 \pm 0.01 (5)	1.01 \pm 0.04	1.04 \pm 0.03 (5)	1.00 \pm 0.03	1.02 \pm 0.02 (6)	1.00 \pm 0.02 (7)

4. Discussion

4.1. Processes driving porewater chemistry

This study shows that Barataria Basin porewaters have some of the highest reported DIC and TA concentrations for coastal marshes (Wang et al., 2016; Taillardat et al., 2018a, 2018b; Guimond et al., 2020; Santos et al., 2021). This could be a combination of high organic matter remineralization rates and microtidal environment. The diurnal tidal range is only 0.35 m at the coast and decreases by an order of magnitude as the tide progresses inland (Das et al., 2012). This low tidal range coupled with low surface elevation of these marshes can result in longer residence time of porewater leading to the high DIC and TA

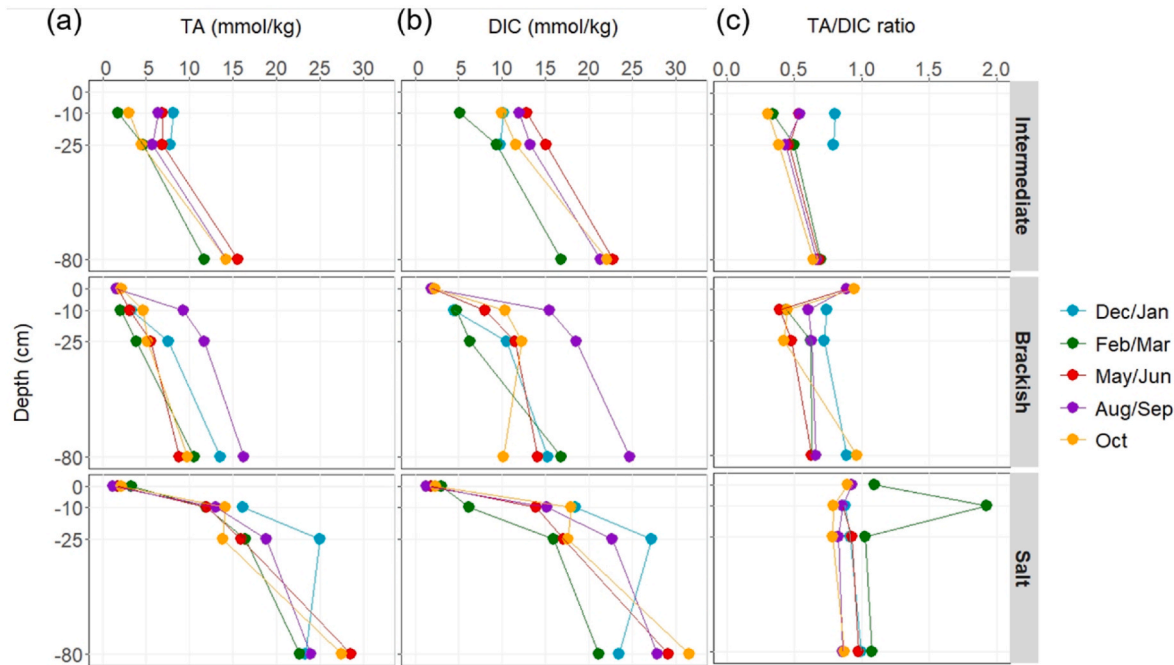


Fig. 4. Porewater TA (a), DIC (b), and TA/DIC ratio during the five field trips. Colder (blue and green) and warmer (red, purple, and yellow) colors were used to represent colder (December to March) and warmer (May to October) months. Depth = -10, -25, and -80 cm were used to denote porewater sampling depth of 10, 25, and 80 cm below the marsh surface. Depth = 0 cm was used to denote water samples collected on the marsh surface. Marsh surface was not flooded if there is no data for depth = 0 cm. (For interpretation of the references to color in this figure legend, the reader is referred to the Web version of this article.)

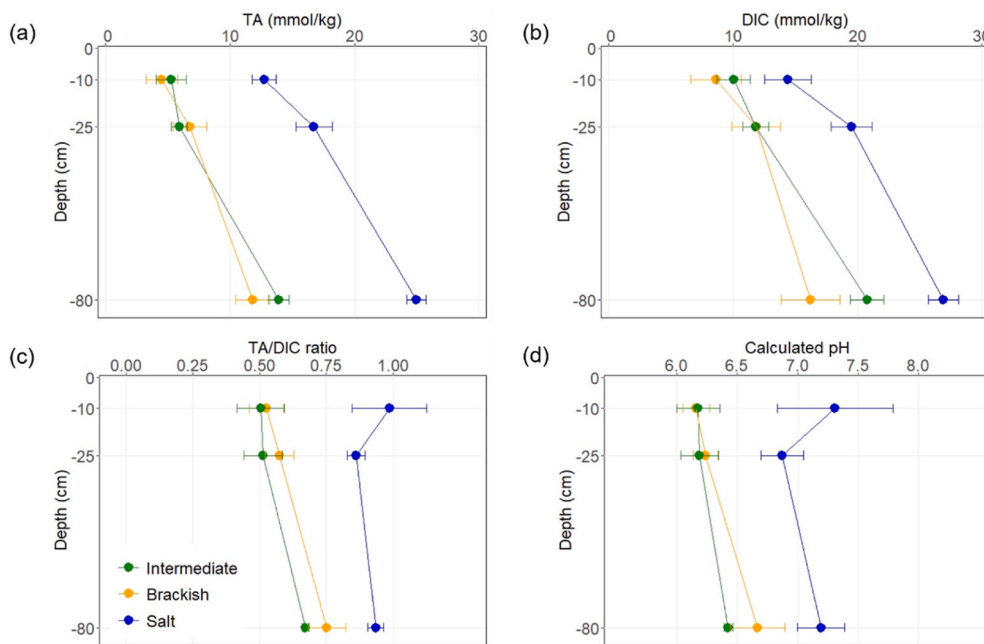


Fig. 5. Mean and standard errors of TA (a), DIC (b), TA/DIC ratio (c), and calculated pH (d) in the three marshes. Mean values are represented by solid dots, and the horizontal bars represent standard errors. Depth = -10, -25, and -80 cm were used to denote porewater sampling depth of 10, 25, and 80 cm below the marsh surface. (For interpretation of the references to color in this figure legend, the reader is referred to the Web version of this article.)

concentrations observed in these three marshes.

The TA/DIC ratios in the intermediate and brackish marshes of Barataria Bay were similar and lower than in the salt marsh (Fig. 5c), suggesting the dominant microbial processes may differ in the three marshes. The porewater TA/DIC ratios of the salt marsh edge and interior sites were different at shallower depths but converged with depth at 80 cm possibly due to less hydrologic exchange (Fig. 6), suggesting that similar biogeochemical processes might be controlling soil TA and DIC at the marsh edge and interior and that there could be considerable exchange of tidal water in the upper layers but not at 80 cm.

The relationship between DIC and alkalinity can provide insights into the biogeochemical drivers of DIC and alkalinity dynamics (Borges, 2003; Bouillon et al., 2007). The ratio of TA to DIC tends to follow a stoichiometric relationship specific to the pathways of organic matter mineralization. TA and DIC concentrations are often normalized for surface water with widely diverging salinity (Friis et al., 2003; Sippo et al., 2016), but normalizing porewater TA and DIC data in marshes with differing salinities is difficult to carry out with relatively fewer samples and varying biogeochemical processes with depth. Therefore, we did not normalize our TA and DIC concentrations and did not combine porewater samples from the three different marshes in our analysis. Results showed that DIC and TA were strongly correlated at all three marshes, with the regression slopes indicating the dominance of anaerobic processes driving porewater DIC and TA. Slopes ranged from 0.614 to 0.855 (Fig. 7), similar to slopes expected for a combination of aerobic respiration (-0.2), denitrification (0.8), sulfate reduction (1.0), and iron reduction (8.0). The redox potentials measured at these three marshes support such processes (Fig. 3c). Sulfate reduction is usually a dominant respiration process in salt marshes due to the abundance of sulfate (Cai et al., 2003a; Burdige, 2011). The slopes of the intermediate and brackish marshes were lower than the salt marsh (Fig. 7), which is probably due to the sulfate reduction occurring in the salt marsh. The higher sulfate reduction rate in the salt marsh could also potentially explain the higher DIC and TA concentrations in the salt marsh than in the other two marshes. The observed TA/DIC ratio of porewater alone cannot provide sufficient information about the dominant respiration

pathway in these marshes. We can only speculate based on previous approaches that have used the Redfield ratio as a starting point to understand the contributions of various respiration processes in marsh soil DIC and TA (Krumins et al., 2013; Sippo et al., 2016). High nitrate concentrations of up to 82 $\mu\text{mol/L}$ have been reported from the Barataria Bay region, which resulted in high denitrification rates of 21.4–900 $\mu\text{mol N m}^{-2} \text{hr}^{-1}$ (Yu et al., 2006; VanZomeren et al., 2013; Vaccare et al., 2019; Upreti et al., 2021; Turner et al., 2019). Thus, denitrification has an important impact on the observed porewater TA/DIC ratio than other respiration pathways, especially in the intermediate and brackish marshes where average salinities in the adjacent channels and creeks are 1 and 3, respectively. In case of the salt marsh, which has an average salinity of 7 in the adjacent channel and creek, the anaerobic respiration is probably a more complex interplay of sulfate reduction and denitrification depending on the seasonal freshwater influence. It must be noted here that only denitrification results in production of more DIC than TA, i.e., $\text{TA/DIC} < 1$, while other anaerobic respiration pathways including manganese, iron, and sulfate reductions result in TA/DIC ratios greater than 1 (Table 1). However, calcium carbonate precipitation in the porewater cannot be ruled out given high DIC and TA concentrations and likely high carbonate saturation state in the anoxic porewater (Boudreau and Canfield, 1993; Lin et al., 2020). Ca^{+2} concentrations in porewater from our study site are not available but porewater analysis in other coastal Louisiana marshes indicate Ca^{+2} concentrations ranging from 2.5 to 12.5 mM (Robert P. Gambrell, Louisiana State University, personal communication). Thus, the influence of calcium carbonate precipitation on TA/DIC ratio in the porewater cannot be ignored.

A positive relationship was observed between DIC and porewater sampling depth for all three marshes (Figs. 4 and 5). Similarly, TA concentrations increased with depth. These relationships, in combination with the slopes of DIC versus TA correlations, are indicative of sediment anaerobic processes, suggesting that exchange between marsh and adjacent surface water could be a driver of inorganic carbon exchange. This is supported by previous studies in mangroves and marshes that have suggested that tidal pumping drives high surface water inorganic carbon concentrations through high porewater exchange rates

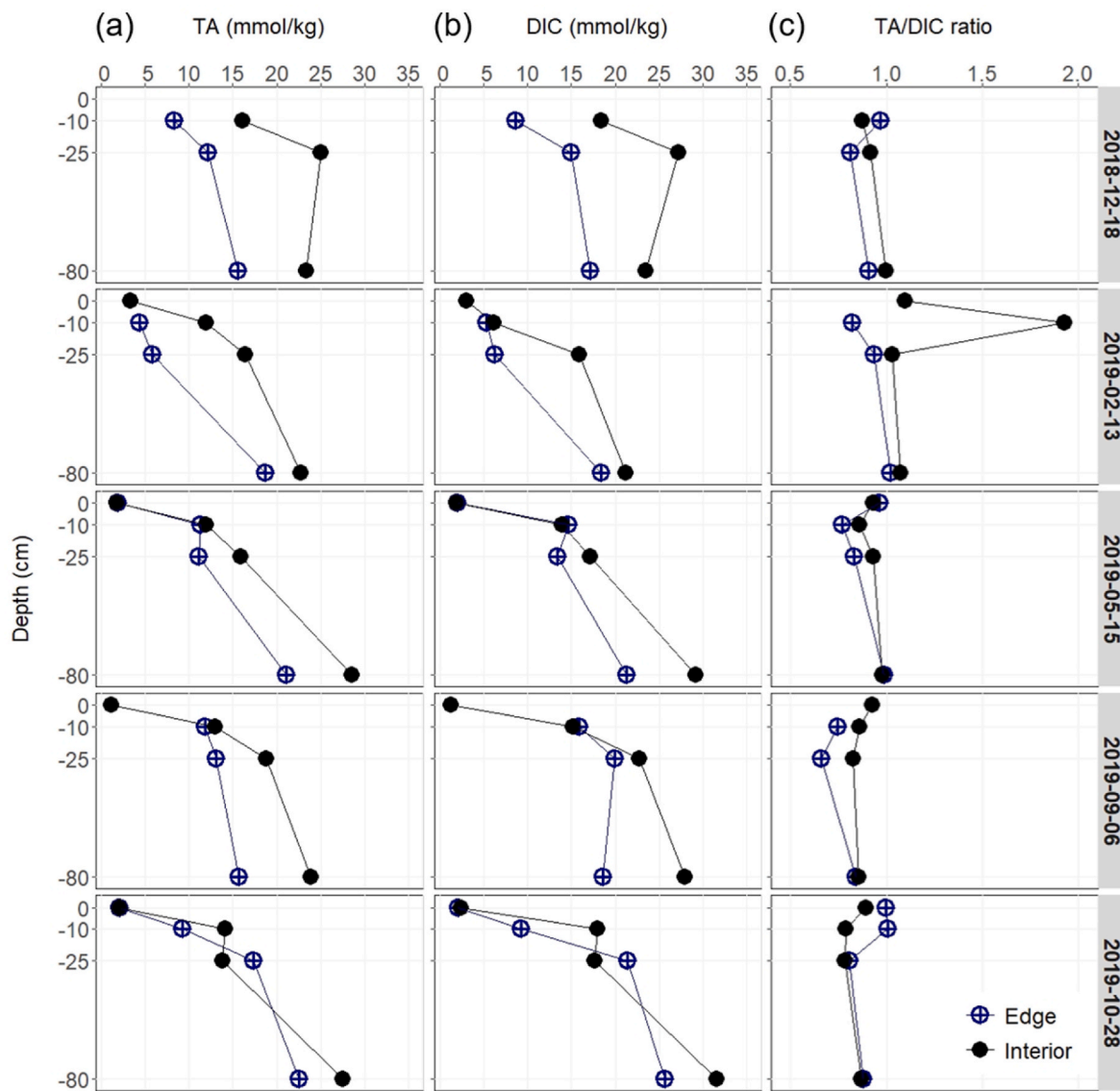


Fig. 6. Salt marsh edge (blue circles with crosses) and interior (black dots) porewater TA (a), DIC (b), and TA/DIC during the five field trips. Depth = -10, -25, and -80 cm were used to denote porewater sampling depth of 10, 25, and 80 cm below the marsh surface. Depth = 0 cm was used to denote water samples collected on the marsh surface. Marsh surface was not flooded if there is no data for depth = 0 cm. (For interpretation of the references to color in this figure legend, the reader is referred to the Web version of this article.)

(Maher et al., 2013; Wang and Cai, 2004; Wang et al., 2016). High TA and DIC exports driven by porewater exchange have been reported for a number of coastal systems (e.g., Faber et al., 2014; Santos et al., 2015; Stewart et al., 2015; Burt et al., 2016; Sippo et al., 2016; Taillardat et al., 2018a), including coastal wetlands (Cai et al., 2000; Neubauer and Anderson, 2003; Wang and Cai, 2004; Wang et al. 2016, 2018; Najjar et al., 2018; Santos et al., 2019). The high porewater concentrations of DIC and TA reported in this study suggest that this could be a substantial source of TA and DIC exported to the coastal ocean under increased hydrological exchanges between marsh soil and surrounding surface water that can occur due to high frequency storms as well as future tidal regime changes caused by sea level rise and/or land loss (Kindinger et al., 2013).

Temperature and flooding could also play important roles in marsh biogeochemical processes. Our results showed that TA and DIC concentrations were generally higher during warmer months (Fig. 4). Since decomposition rates are faster at higher temperatures (Roberts and Doty, 2015), we expected to see higher porewater TA and DIC concentrations during warmer months. However, we suspect flooding

conditions also played an important role. When a marsh has no overlying water, higher organic matter respiration rates can be expected because of oxygen availability in the soil upper layers, which could mean higher DIC but not higher TA (Table 1). Therefore, this cannot sufficiently explain the higher TA and DIC observed in the salt marsh at 10 and 25 cm during that period. Low water level in winter and the microtidal environment can limit lateral exchange leading to buildup of DIC and TA over time. This can explain the higher TA and DIC in the salt marsh porewater in December when soil respiration rate is expected to be lower.

4.2. Impact of marsh type on coastal acidification

Our results show that the channel and creek surface waters near all three marshes had TA/DIC ratios close to 1 (Table 3), implying that $[CO_2] \approx [CO_3^{2-}]$, and that the buffering capacities of the channels and creeks are low (Wang et al., 2016). The ratio of TA to DIC concentrations indicate the relative abundance of carbonate species (e.g., CO_2 and CO_3^{2-}) in coastal waters. For specific salinity and temperature ranges,

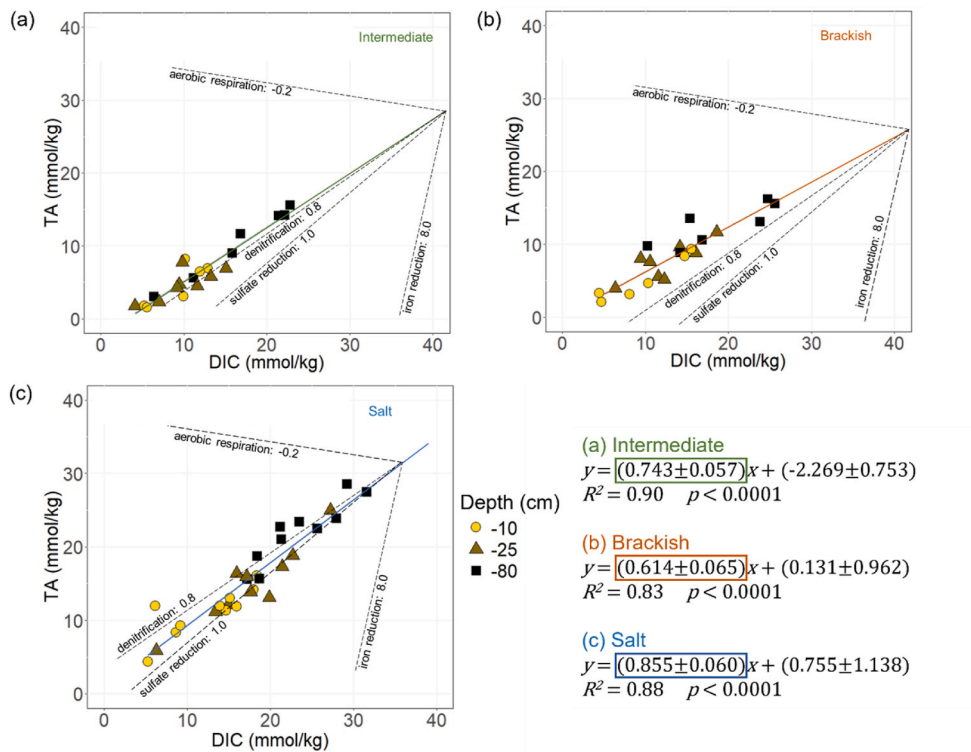


Fig. 7. Correlations of DIC versus TA at three marshes in Barataria Basin, Louisiana. Both marsh edge and interior data are included. Solid green, orange, and blue lines indicate linear correlations, and dashed black lines indicate stoichiometric ratios of the biogeochemical processes that can control TA and DIC. Slopes of the regression equations are highlighted using a colored rectangular box. (For interpretation of the references to color in this figure legend, the reader is referred to the Web version of this article.)

the ratio of TA/DIC can be closely correlated with carbonate system parameters, such as Ω_A and pH (Xue and Cai, 2020). As such, TA and DIC ratio has been widely utilized in studies of coastal carbonate chemistry (e.g., Wang et al., 2013; Mol et al., 2018). Different TA/DIC ratios can imply a difference in buffer capacity. Porewater TA/DIC ratios in all three marshes were less than 1, with the salt marsh having higher TA/DIC ratios than the intermediate and brackish marshes (Fig. 4c). The differences in porewater and surface water TA/DIC ratios suggests that exchange between porewater and surface water could decrease the buffering capacity and pH in these systems. This contrasts with several studies on mangroves, which have shown higher TA than DIC resulting in enhanced buffering capacity of surrounding water bodies through hydraulic exchange (Sippo et al., 2016; Saderne et al., 2019; Akhand et al., 2021). We attribute this difference to denitrification as well as carbonate precipitation, both of which will result in a TA/DIC ratio less than 1 in the marsh soil.

The CO₂ fixed by marsh vegetation and the subsequent export of inorganic and organic carbon is an important process that causes the marsh-influenced nearshore and offshore coastal regions to be annual net sources of atmospheric CO₂ (Cai et al., 2003b; Wang and Cai, 2004; Borges et al., 2005). Studies have also shown that the export of inorganic carbon from coastal marshes to coastal ocean is substantial and could play an important role on coastal acidification (Cai et al., 2000; Wang et al., 2016; Laurent et al., 2017). The addition of DIC (CO₂) to the typical coastal water will initially decrease then increase buffering capacity depending on the TA and DIC ratio. During this process, pH always decreases regardless of buffering capacity changes, as pH change is dominated by inputs of CO₂ (Wang et al., 2016). Therefore, changes in surface water TA/DIC due to marsh porewater inputs can directly alter the sensitivity of coastal water pH. In our study, porewater TA/DIC ratios of all three marshes were generally less than 1 (Fig. 4c), suggesting that an input of these porewaters could decrease the channel and creek's TA/DIC ratio (Table 3), which in turn would influence the buffering capacity and pH of channels and creeks. For porewater to have substantial influence, it needs to undergo active exchange and be laterally transported to surrounding surface waters, such as tidal channels and

creeks.

The exchange rate between marsh soil and surrounding channels and creeks plays an important role in porewater and surface water TA/DIC ratios. Higher rate of exchange could increase the TA/DIC ratio in porewater and decrease the TA/DIC ratio in the creeks and channels. Instead, the salt marsh soils had the highest TA/DIC ratios. A possible explanation is that the hydrological differences between the salt marsh and the intermediate and brackish marshes play an important role. The salt marsh has daily flooding and ebbing as part of the tidal signal, which should lead to higher exchange between porewater and adjacent surface water, which would result in higher porewater TA/DIC ratios than the two lower salinity marshes. Our study of inorganic carbon dynamics in three marshes with contrasting salinity may provide valuable insight on TA/DIC ratios and potential ocean acidification if lower salinity marshes transition to more saline marshes as might be expected with increases in rates of sea level rise.

Our study did not show any correlation between porewater TA/DIC ratio and the TA/DIC ratio of surface water in the surrounding creeks and channels, which were around 1 (Table 3). This study was designed to understand whether porewater endmembers can potentially influence the acidification of the surrounding water by studying the seasonal changes in porewater DIC and TA in contrasting marshes. It is consequently difficult to extrapolate the extent of the porewater TA/DIC impact on surrounding water bodies. The extent of exchange between marsh porewater and surrounding water bodies will determine the influence of porewater on surrounding water bodies which in turn depends on several processes such as hydrology, tide, and wind speed/direction. Thus, a detailed time-series study of such porewater exchange would offer insight on its impacts to adjacent water bodies, which was beyond the scope of our current study. Our results showing TA/DIC < 1 in the majority of our porewater samples across different seasons indicate that there is a distinct possibility for porewater to potentially influence the carbonate chemistry of the surrounding water. There are no prior estimates of porewater DIC and TA concentrations reported from our study region. When compared with other regions in the world (Taillardat et al., 2018a, 2018b), porewater TA and DIC in our study

sites are among the highest and were up to 15 times higher than surrounding surface water. Such high TA and DIC concentrations suggest either low exchange rates between marsh soils and surrounding water bodies leading to the accumulation of TA and DIC, a very high organic decomposition rate in our marsh soils, or a combination of both. The coastal marshes in this region are currently undergoing rapid erosion (Snedden et al., 2007; Couvillon et al., 2017), and marsh loss could potentially release high DIC and low pH porewater to adjacent estuaries. With TA/DIC ratios so close to 1 in the surface water, even a very small change in CO_2 addition could dramatically change the pH and buffering capacity of coastal waters, which could have complex implications for coastal ocean in the future (Cai et al., 2011; Wang et al., 2016).

Porewater pH at all three marshes were lower than the pH of corresponding channels and creeks (Table 3 and Fig. 3). Marsh loss in coastal Louisiana will potentially increase the exchange rate (Kindinger et al., 2013) between marsh soil and coastal surface water bodies resulting in the delivery of porewater with low pH and low TA/DIC into the already stressed northern Gulf of Mexico (Ekstrom et al., 2015). The resulting coastal acidification from such a process could be harmful to fisheries and marine wildlife (Kleypas et al., 1999; Feely et al., 2018).

The study was conducted during an extended period of low salinity across Barataria Basin. The processes and observations could change if the sampling had been done in years with extended droughts such as 2000 and 2006. The extent to which our results would change is unclear. Unfortunately, there is little to no information on such subjects currently to help us be more certain as this is the first study in this region to attempt to understand inorganic carbon dynamics in marsh soils with contrasting salinity. Future studies could focus on the exchange of porewater between marsh and adjacent water bodies, and the porewater data reported in this study suggests that such exchange processes can have implications for coastal acidification.

5. Conclusions

This study investigated the spatial and temporal trends of dissolved inorganic carbon (DIC) and total alkalinity (TA) and their ratio in three marshes with contrasting salinity within Barataria Basin, Louisiana, USA. It is the first study on the spatiotemporal trend of porewater carbonate chemistry in this region. Porewater TA and DIC concentrations in our study sites are among the highest if it is not the highest when compared with previous studies and were up to 15 times higher than surrounding surface water bodies. Such high TA and DIC concentrations suggest either low exchange rates between marsh soils and surrounding water bodies leading to the accumulation of TA and DIC, or a very high organic decomposition rate in our marsh soils, or a combination of both. The TA concentrations were found to be usually lower than porewater DIC, suggesting that marshes in coastal Louisiana, including salt marshes, can be potential drivers of coastal acidification because of the dominant denitrification pathway associated with high nitrate load in this region. Future studies of coastal ocean acidification could also consider not only atmospheric pCO_2 and temperature changes, but also incorporate the effects of coastal systems, including marshes and associated DIC and TA inputs, which are expected to increase due to wetland loss and eutrophication (Cai et al., 2011; Sunda and Cai, 2012; Laurent et al., 2017). The spatial and temporal characterizations of the porewater DIC and TA depth profiles could help constrain mass balance models of marsh DIC and TA inputs and enhance our understanding of the marsh carbon pump in coastal oceans.

CRediT authorship contribution statement

Songjie He: Conceptualization, Formal analysis, Investigation, Methodology, Visualization, Writing – original draft, Writing – review & editing. **Kanchan Maiti:** Writing – review & editing, Resources, Methodology, Funding acquisition, Conceptualization. **Christopher M. Swarzenski:** Funding acquisition, Investigation, Methodology,

Resources, Writing – review & editing. **Tracy Elsey-Quirk:** Writing – review & editing, Funding acquisition, Resources. **Gina N. Groseclose:** Investigation, Writing – review & editing. **Dubravko Justic:** Writing – review & editing, Funding acquisition.

Declaration of competing interest

The authors declare that they have no known competing financial interests or personal relationships that could have appeared to influence the work reported in this paper.

Acknowledgement

This work is supported by the NSF Chemical Oceanography program (award# OCE-1756788 to Kanchan Maiti), the U.S. Department of the Treasury RESTORE Act Centers of Excellence (award# CPRA-2015-COE-JE to Tracy Quirk), and by the U.S. Geological Survey Ecosystems Program, South Central Climate Adaptation Science Center. The first author is grateful for the inspiration and support provided by the many long conversations with Naomi Cohen. The authors thank the editors and anonymous reviewers for their careful readings of the manuscript and constructive suggestions. There are no conflicts of interest with members of the editorial board. Any use of trade, firm, or product names is for descriptive purposes only and does not imply endorsement by the U.S. Government.

Appendix A. Supplementary data

Supplementary data to this article can be found online at <https://doi.org/10.1016/j.ecss.2022.107801>.

References

- Akhand, A., Watanabe, K., Chanda, A., Tokoro, T., Chakraborty, K., Moki, H., Tanaya, T., Ghosh, J., et al., 2021. Lateral carbon fluxes and CO_2 evasion from a subtropical mangrove-seagrass-coral continuum. *Sci. Total Environ.* 752, 142190. <https://doi.org/10.1016/j.scitotenv.2020.142190>.
- Anderson, M.M., Maiti, K., Xue, Z.G., Ou, Y., 2020. Dissolved inorganic carbon transport in the surface-mixed layer of the Louisiana shelf in northern Gulf of Mexico. *J. Geophys. Res.: Oceans* 125. <https://doi.org/10.1029/2020jc016605>.
- Baker, R., Taylor, M.D., Able, K.W., Beck, M.W., Cebran, J., Colombano, D.D., Connolly, R.M., Curran, C., et al., 2020. Fisheries rely on threatened salt marshes. *Science* 370, 670. <https://doi.org/10.1126/science.abe9332>.
- Bauer, J.E., Cai, W.-J., Raymond, P.A., Bianchi, T.S., Hopkinson, C.S., Regnier, P.A.G., 2013. The changing carbon cycle of the coastal ocean. *Nature* 504, 61. <https://doi.org/10.1038/nature12857>.
- Bogard, M.J., Bergamaschi, B.A., Butman, D.E., Anderson, F., Knox, S.H., Windham-Myers, L., 2020. Hydrologic export is a major component of coastal wetland carbon budgets. *Global Biogeochem. Cycles* 34. <https://doi.org/10.1029/2019gb006430>.
- Borges, A.V., 2003. Atmospheric CO_2 flux from mangrove surrounding waters. *Geophys. Res. Lett.* 30. <https://doi.org/10.1029/2003gl017143>.
- Borges, A.V., Delille, B., Frankignoulle, M., 2005. Budgeting sinks and sources of CO_2 in the coastal ocean: diversity of ecosystems counts. *Geophys. Res. Lett.* 32. <https://doi.org/10.1029/2005gl023053> n/a-n/a.
- Boudreau, B.P., Canfield, D.E., 1993. A Comparison of Closed- and Open-System Models for Porewater pH and Calcite-Saturation State. [https://doi.org/10.1016/0016-7037\(93\)90434-X](https://doi.org/10.1016/0016-7037(93)90434-X).
- Bouillon, S., Dehairs, F., Velimirov, B., Abril, G., Borges, A.V., 2007. Dynamics of organic and inorganic carbon across contiguous mangrove and seagrass systems (Gazi Bay, Kenya). *J. Geophys. Res.* 112. <https://doi.org/10.1029/2006jg000325>.
- Burdige, D.J., 2011. *Estuarine and coastal Sediments – coupled biogeochemical cycling*. Treatise-Estuar. Coast. Sci. 279–316.
- Burt, W.J., Thomas, H., Hagens, M., Pätsch, J., Clargo, N.M., Salt, L.A., Winde, V., Böttcher, M.E., 2016. Carbon sources in the North Sea evaluated by means of radium and stable carbon isotope tracers. *Limnol. Oceanogr.* 61, 666–683. <https://doi.org/10.1002/lnco.10243>.
- Cai, W.-J., Hu, X., Huang, W.-J., Murrell, M.C., Lehrter, J.C., Lohrenz, S.E., Chou, W.-C., Zhai, W., et al., 2011. Acidification of subsurface coastal waters enhanced by eutrophication. *Nat. Geosci.* 4, 766–770. <https://doi.org/10.1038/ngeo1297>.
- Cai, W.-J., Wang, Y., Hodson, R.E., 1998. Acid-base properties of dissolved organic matter in the estuarine waters of Georgia, USA. *Geochem. Cosmochim. Acta* 62, 473–483. [https://doi.org/10.1016/S0016-7037\(97\)00363-3](https://doi.org/10.1016/S0016-7037(97)00363-3).
- Cai, W.-J., Wang, Y., Krest, J., Moore, W.S., 2003a. The geochemistry of dissolved inorganic carbon in a surficial groundwater aquifer in North Inlet, South Carolina, and the carbon fluxes to the coastal ocean. *Geochem. Cosmochim. Acta* 67, 631–639. [https://doi.org/10.1016/s0016-7037\(02\)01167-5](https://doi.org/10.1016/s0016-7037(02)01167-5).

Cai, W.-J., Wang, Z.A., Wang, Y., 2003b. The role of marsh-dominated heterotrophic continental margins in transport of CO₂ between the atmosphere, the land-sea interface and the ocean. *Geophys. Res. Lett.* 30 <https://doi.org/10.1029/2003gl017633>.

Cai, W.-J., Wiebe, W.J., Wang, Y., Sheldon, J.E., 2000. Intertidal marsh as a source of dissolved inorganic carbon and a sink of nitrate in the Satilla River estuarine complex in the southeastern U.S. *Limnol. Oceanogr.* 45, 1743–1752. <https://doi.org/10.4319/lo.2000.45.8.1743>.

Cai, W.J., 2011. Estuarine and coastal ocean carbon paradox: CO₂ sinks or sites of terrestrial carbon incineration? *Ann. Rev. Mar. Sci.* 3, 123–145. <https://doi.org/10.1146/annurev-marine-120709-142723>.

Chmura, G.L., Anisfeld, S.C., Cahoon, D.R., Lynch, J.C., 2003. Global carbon sequestration in tidal, saline wetland soils. *Global Biogeochem. Cycles* 17. <https://doi.org/10.1029/2002gb001917> n/a-n/a.

Couvillion, B.R., Beck, H., Schoolmaster, D., Fischer, M., 2017. Land area change in coastal Louisiana (1932 to 2016). *Pam.accompany.U.S. Geol. Surv. Invest. Map 3381, p16.* <https://doi.org/10.3133/sim3381>.

CPRA (Coastal Protection, Restoration Authority, 2017. Louisiana's Comprehensive Master Plan for a Sustainable Coast. <http://coastal.la.gov/our-plan/2017-coastal-master-plan/>. (Accessed 1 February 2022).

Das, A., Justic, D., Inoue, M., Hoda, A., Huang, H., Park, D., 2012. Impacts of Mississippi River diversions on salinity gradients in a deltaic Louisiana estuary: ecological and management implications. *Estuar. Coast Shelf Sci.* 111, 17–26. <https://doi.org/10.1016/j.ecss.2012.06.005>.

Dickson, A.G., 1990. Standard potential of the reaction: AgCl(s) + 1/2H₂(g) = Ag(s) + HCl(aq), and the standard acidity constant of the ion HSO₄⁻ in synthetic seawater from 273.15 to 318.15 K. *J. Chem. Thermodyn.* 22, 113–127. [https://doi.org/10.1016/0021-9614\(90\)90074-Z](https://doi.org/10.1016/0021-9614(90)90074-Z).

Dickson, A., 2010. Standards for ocean measurements. *Oceanography* 23, 34–47. <https://doi.org/10.5670/oceanog.2010.22>.

Downing, B.D., Boss, E., Bergamaschi, B.A., Fleck, J.A., Lionberger, M.A., Ganju, N.K., Schoellhamer, D.H., Fujii, R., 2009. Quantifying fluxes and characterizing compositional changes of dissolved organic matter in aquatic systems in situ using combined acoustic and optical measurements. *Limnol. Oceanogr. Methods* 7, 119–131. <https://doi.org/10.4319/lom.2009.7.119>.

Duarte, C.M., Middelburg, J.J., Caraco, N., 2005. Major role of marine vegetation on the oceanic carbon cycle. *Biogeosciences* 2, 1–8. <https://doi.org/10.5194/bg-2-1-2005>.

Ekstrom, J.A., Suatoni, L., Cooley, S.R., Pendleton, L.H., Waldbusser, G.G., Cinner, J.E., Ritter, J., Langdon, C., et al., 2015. Vulnerability and adaptation of US shellfisheries to ocean acidification. *Nat. Clim. Change* 5, 207–214. <https://doi.org/10.1038/nclimate2508>.

Elsey-Quirk, T., Seliskar, D.M., Sommerfield, C.K., Gallagher, J.L., 2011. Salt marsh carbon pool distribution in a mid-Atlantic lagoon, USA: sea level rise implications. *Wetlands* 31, 87–99. <https://doi.org/10.1007/s13157-010-0139-2>.

Faber, P.A., Evrard, V., Woodland, R.J., Cartwright, I.C., Cook, P.L.M., 2014. Pore-water exchange driven by tidal pumping causes alkalinity export in two intertidal inlets. *Limnol. Oceanogr.* 59, 1749–1763. <https://doi.org/10.4319/lo.2014.59.5.1749>.

Feeley, R.A., Okazaki, R.R., Cai, W.-J., Bednaršek, N., Alin, S.R., Byrne, R.H., Fassbender, A., 2018. The combined effects of acidification and hypoxia on pH and aragonite saturation in the coastal waters of the California current ecosystem and the northern Gulf of Mexico. *Continent. Shelf Res.* 152, 50–60. <https://doi.org/10.1016/j.csr.2017.11.002>.

Friis, K., Körtzinger, A., Wallace, D.W.R., 2003. The salinity normalization of marine inorganic carbon chemistry data. *Geophys. Res. Lett.* 30 <https://doi.org/10.1029/2002gl015898>.

Ganju, N.K., Hayn, M., Chen, S.-N., Howarth, R.W., Dickhut, P.J., Aretxabaleta, A.L., Marino, R., 2012. Tidal and groundwater fluxes to a shallow, microtidal estuary: constraining inputs through field observations and hydrodynamic modeling. *Estuar. Coast* 35, 1285–1298. <https://doi.org/10.1007/s12237-012-9515-x>.

Gran, G., 1952. Determination of the equivalence point in potentiometric titrations. Part II. *Analyst* 77, 661–671. <https://doi.org/10.1039/AN9527700661>.

Guimond, J.A., Seyfferth, A.L., Moffett, K.B., Michael, H.A., 2020. A physical-biogeochemical mechanism for negative feedback between marsh crabs and carbon storage. *Environ. Res. Lett.* 15 (3) <https://doi.org/10.1088/1748-9326/ab60e2>.

Hayes, M.P., Sapkota, Y., White, J.R., Cook, R.L., 2021. Investigating the impact of in situ soil organic matter degradation through porewater spectroscopic analyses on marsh edge erosion. *Chemosphere* 268, 129266. <https://doi.org/10.1016/j.chemosphere.2020.129266>.

Herke, W.H., 1995. Natural fisheries, marsh management, and mariculture: complexity and conflict in Louisiana. *Estuaries* 18, 10–17. <https://doi.org/10.2307/1352279>.

Hu, X., Cai, W.-J., 2011. An assessment of ocean margin anaerobic processes on oceanic alkalinity budget. *Global Biogeochem. Cycles* 25. <https://doi.org/10.1029/2010gb003859> n/a-n/a.

Kindinger, J.L., Buster, N.A., Flocks, J.G., Bernier, J.C., Kulp, M.A., 2013. Louisiana Barrier Island Comprehensive Monitoring (BICM) Program Summary Report: Data and Analyses 2006 through 2010: U.S. Geological Survey Open-File Report 2013-1083, p. 86. <http://pubs.usgs.gov/of/2013/1083/>. (Accessed 1 February 2022).

Kleypas, J.A., Buddemeier, R.W., Archer, D., Gattuso, J.-P., Langdon, C., Odyke, B.N., 1999. Geochemical consequences of increased atmospheric carbon dioxide on coral reefs. *Science* 284, 118. <https://doi.org/10.1126/science.284.5411.118>.

Kolker, A.S., Allison, M.A., Hameed, S., 2011. An evaluation of subsidence rates and sea-level variability in the northern Gulf of Mexico. *Geophys. Res. Lett.* 38 <https://doi.org/10.1029/2011gl049458> n/a-n/a.

Krumins, V., Gehlen, M., Arndt, S., Van Cappellen, P., Regnier, P., 2013. Dissolved inorganic carbon and alkalinity fluxes from coastal marine sediments: model estimates for different shelf environments and sensitivity to global change. *Biogeosciences* 10, 371–398. <https://doi.org/10.5194/bg-10-371-2013>.

Laurent, A., Fennel, K., Cai, W.-J., Huang, W.-J., Barbero, L., Wanninkhof, R., 2017. Eutrophication-induced acidification of coastal waters in the northern Gulf of Mexico: insights into origin and processes from a coupled physical-biogeochemical model. *Geophys. Res. Lett.* 44, 946–956. <https://doi.org/10.1002/2016gl071881>.

Lin, C.Y., Turchyn, A.V., Krylov, A., Antler, G., 2020. The microbially driven formation of siderite in salt marsh sediments. *Geobiology* 18 (2), 207–224. <https://doi.org/10.1111/gbi.12371>.

Linscombe, R.G., Hartley, S.B., 2011. Analysis of Change in Marsh Types of Coastal Louisiana, 1978–2001: U.S. Geological Survey Open-File Report 2010-1282, p. 52. <https://pubs.usgs.gov/of/2010/1282/pdf/OF2010-1282.pdf>. (Accessed 1 February 2022).

Maher, D.T., Santos, I.R., Golsby-Smith, L., Gleeson, J., Eyre, B.D., 2013. Groundwater-derived dissolved inorganic and organic carbon exports from a mangrove tidal creek: the missing mangrove carbon sink? *Limnol. Oceanogr.* 58, 475–488. <https://doi.org/10.4319/lo.2013.58.2.0475>.

McKee, K.L., Mendelsohn, I.A., Hester, M.W., 1988. Reexamination of pore water sulfide concentrations and redox potentials near the aerial roots of rhizophora mangle and avicennia germinans. *Am. J. Bot.* 75 (9), 1352–1359. <https://doi.org/10.1002/j.1537-2197.1988.tb14196.x>.

McLeod, E., Chmura, G.L., Bouillon, S., Salm, R., Björk, M., Duarte, C.M., Lovelock, C.E., Schlesinger, W.H., et al., 2011. A blueprint for blue carbon: toward an improved understanding of the role of vegetated coastal habitats in sequestering CO₂. *Front. Ecol. Environ.* 9, 552–560. <https://doi.org/10.1890/110004>.

Miller, F.J., Graham, T.B., Huang, F., Bustos-Serrano, H., Pierrot, D., 2006. Dissociation constants of carbonic acid in seawater as a function of salinity and temperature. *Mar. Chem.* 100, 80–94. <https://doi.org/10.1016/j.marchem.2005.12.001>.

Mol, J., Thomas, H., Myers, P.G., Hu, X., Mucci, A., 2018. Inorganic carbon fluxes on the mackenzie shelf of the beaufort sea. *Biogeoosciences* 15, 1011–1027. <https://doi.org/10.5194/bg-15-1011-2018>.

Najjar, R.G., Herrmann, M., Alexander, R., Boyer, E.W., Burdige, D.J., Butman, D., Cai, W.J., Canuel, E.A., et al., 2018. Carbon budget of tidal wetlands, estuaries, and shelf waters of eastern North America. *Global Biogeochem. Cycles* 32, 389–416. <https://doi.org/10.1002/2017gb005790>.

Neubauer, S.C., Anderson, I.C., 2003. Transport of dissolved inorganic carbon from a tidal freshwater marsh to the York River estuary. *Limnol. Oceanogr.* 48, 299–307. <https://doi.org/10.4319/lo.2003.48.1.0299>.

Peyronnin, N., Caffey, R., Cowan, J., Justic, D., Kolker, A., Laska, S., McCorquodale, A., Melancon, E., et al., 2017. Optimizing sediment diversion operations: working group recommendations for integrating complex ecological and social landscape interactions. *Water* 9. <https://doi.org/10.3390/w9060368>.

Pierrot, D., Lewis, E., Wallace, D.W.R., 2006. MS Excel Program Developed for CO₂ System Calculations. ORNL/CDIAC-105a. Carbon Dioxide Information Analysis Center. Oak Ridge National Laboratory, U.S. Department of Energy, Oak Ridge, Tennessee. https://doi.org/10.3334/CDIAC/otg.CO2SYS_XLS_CDIA105a.

Raymond, P.A., Bauer, J.E., Cole, J.J., 2000. Atmospheric CO₂ evasion, dissolved inorganic carbon production, and net heterotrophy in the York River estuary. *Limnol. Oceanogr.* 45 (8), 1707–1717. <https://doi.org/10.4319/lo.2000.45.8.1707>.

Robert, A.M., John, A.B., 2011. Hurricane impacts on coastal wetlands: a half-century record of storm-generated features from southern Louisiana. *J. Coast. Res.* 27, 27–43. <https://doi.org/10.2112/JCOASTRES-D-10-00185.1>.

Roberts, B.J., Doty, S.M., 2015. Spatial and temporal patterns of benthic respiration and net nutrient fluxes in the Atchafalaya River delta estuary. *Estuar. Coast* 38, 1918–1936. <https://doi.org/10.1007/s12237-015-9965-z>.

Ryu, J., Liu, K.B., Blanchette, T.A., 2021a. Holocene environmental history of a freshwater wetland in southern Louisiana: a sedimentary record of delta development, coastal evolution and human activity. *J. Quat. Sci.* 36 (6), 980–990. <https://doi.org/10.1002/jqs.3324>.

Ryu, J., Liu, K.B., Blanchette, T.A., McCloskey, T., 2021b. Identifying forcing agents of environmental change and ecological response on the Mississippi River Delta, Southeastern Louisiana. *Sci. Total Environ.* 794, 148730. <https://doi.org/10.1016/j.scitotenv.2021.148730>.

Saderne, V., Baldry, K., Anton, A., Agusti, S., Duarte, C.M., 2019. Characterization of the CO₂ system in a coral reef, a seagrass meadow, and a mangrove forest in the central Red Sea. *J. Geophys. Res.: Oceans* 124, 7513–7528. <https://doi.org/10.1029/2019JC015266>.

Santos, I.R., Beck, M., Brumsack, H.-J., Maher, D.T., Dittmar, T., Waska, H., Schnetger, B., 2015. Porewater exchange as a driver of carbon dynamics across a terrestrial-marine transect: insights from coupled 222 Rn and pCO₂ observations in the German Wadden Sea. *Mar. Chem.* 171, 10–20. <https://doi.org/10.1016/j.marchem.2015.02.005>.

Santos, I.R., Maher, D.T., Larkin, R., Webb, J.R., Sanders, C.J., 2019. Carbon outwelling and outgassing vs. burial in an estuarine tidal creek surrounded by mangrove and saltmarsh wetlands. *Limnol. Oceanogr.* 64, 996–1013. <https://doi.org/10.1002/ln.11090>.

Santos, I.R., Burdige, D.J., Jennerjahn, T.C., Bouillon, S., Cabral, A., Serrano, O., Wernberg, T., et al., 2021. The renaissance of Odum's outwelling hypothesis in 'Blue Carbon' science. *Estuar. Coast Shelf Sci.* 255, 107361. <https://doi.org/10.1016/j.ecss.2021.107361>.

Shen, C., Jin, G., Xin, P., Kong, J., Li, L., 2015. Effects of salinity variations on pore water flow in salt marshes. *Water Resour. Res.* 51, 4301–4319. <https://doi.org/10.1002/2015wr016911>.

Sippo, J.Z., Maher, D.T., Tait, D.R., Holloway, C., Santos, I.R., 2016. Are mangroves drivers or buffers of coastal acidification? Insights from alkalinity and dissolved

inorganic carbon export estimates across a latitudinal transect. *Global Biogeochem. Cycles* 30, 753–766. <https://doi.org/10.1002/2015gb005324>.

Snedden, G.A., Cable, J.E., Wiseman Jr., W.J., 2007. Subtidal sea level variability in a shallow Mississippi River deltaic estuary, Louisiana. *Estuar. Coast* 30, 802–812. <https://doi.org/10.1007/BF02841335>.

Song, S., Wang, Z.A., Gonnea, M.E., Kroeger, K.D., Chu, S.N., Li, D., Liang, H., 2020. An important biogeochemical link between organic and inorganic carbon cycling: effects of organic alkalinity on carbonate chemistry in coastal waters influenced by intertidal salt marshes. *Geochem. Cosmochim. Acta* 275, 123–139. <https://doi.org/10.1016/j.gca.2020.02.013>.

Stewart, B.T., Santos, I.R., Tait, D.R., Macklin, P.A., Maher, D.T., 2015. Submarine groundwater discharge and associated fluxes of alkalinity and dissolved carbon into Moreton Bay (Australia) estimated via radium isotopes. *Mar. Chem.* 174, 1–12. <https://doi.org/10.1016/j.marchem.2015.03.019>.

Still, B.M., Stolt, M.H., 2015. Subaqueous soils and coastal acidification: a hydropedology perspective with implications for calcifying organisms. *Soil Sci. Soc. Am. J.* 79, 407–416. <https://doi.org/10.2136/sssaj2014.09.0366>.

Sunda, W.G., Cai, W.J., 2012. Eutrophication induced CO₂-acidification of subsurface coastal waters: interactive effects of temperature, salinity, and atmospheric PCO(2). *Environ. Sci. Technol.* 46, 10651–10659. <https://doi.org/10.1021/es300626f>.

Taillardat, P., Willemsen, P., Marchand, C., Friess, D.A., Widory, D., Baudron, P., Truong, V.V., Nguyêñ, T.-N., et al., 2018a. Assessing the contribution of porewater discharge in carbon export and CO₂ evasion in a mangrove tidal creek (Can Gio, Vietnam). *J Hyd* 563, 303–318. <https://doi.org/10.1016/j.jhydrol.2018.05.042>.

Taillardat, P., Ziegler, A.D., Friess, D.A., Widory, D., Truong Van, V., David, F., Thành Nho, N., Marchand, C., 2018b. Carbon dynamics and inconstant porewater input in a mangrove tidal creek over contrasting seasons and tidal amplitudes. *Geochem. Cosmochim. Acta* 237, 32–48. <https://doi.org/10.1016/j.gca.2018.06.012>.

Turner, R.E., McClenahan, G., 2018. Reversing wetland death from 35,000 cuts: opportunities to restore Louisiana's dredged canals. *PLoS One* 13, e0207717. <https://doi.org/10.1371/journal.pone.0207717>.

Turner, R.E., Swenson, E.M., Milan, C.S., Lee, J.M., 2019. Spatial variations in Chlorophyll a, C, N, and P in a Louisiana estuary from 1994 to 2016. *Hydrobiologia*. <https://doi.org/10.1007/s10750-019-3918-7>.

Upreti, K., Rivera-Monroy, V.H., Maiti, K., Giblin, A., Geaghan, J.P., 2021. Emerging wetlands from river diversions can sustain high denitrification rates in a coastal delta. *J. Geophys. Res.: Biogeosciences*, e2020JG006217. <https://doi.org/10.1029/2020JG006217>.

Vaccare, J., Meselhe, E., White, J.R., 2019. The denitrification potential of eroding wetlands in Barataria Bay, LA, USA: implications for river reconnection. *Sci. Total Environ.* 686, 529–537. <https://doi.org/10.1016/j.scitotenv.2019.05.475>.

VanZomeren, C.M., White, J.R., DeLaune, R.D., 2013. Ammonification and denitrification rates in coastal Louisiana bayou sediment and marsh soil: implications for Mississippi river diversion management. *Ecol. Eng.* 54, 77–81. <https://doi.org/10.1016/j.ecoleng.2013.01.029>.

Wang, S.R., Di Iorio, D., Cai, W.J., Hopkinson, C.S., 2018. Inorganic carbon and oxygen dynamics in a marsh-dominated estuary. *Limnol. Oceanogr.* 63, 47–71. <https://doi.org/10.1002/lno.10614>.

Wang, Z.A., Cai, W.-J., 2004. Carbon dioxide degassing and inorganic carbon export from a marsh-dominated estuary (the Duplin River): a marsh CO₂ pump. *Limnol. Oceanogr.* 49, 341–354. <https://doi.org/10.4319/lo.2004.49.2.02341>.

Wang, Z.A., Kroeger, K.D., Ganju, N.K., Gonnea, M.E., Chu, S.N., 2016. Intertidal salt marshes as an important source of inorganic carbon to the coastal ocean. *Limnol. Oceanogr.* 61, 1916–1931. <https://doi.org/10.1002/lno.10347>.

Wang, Z.A., Wanninkhof, R., Cai, W.-J., Byrne, R.H., Hu, X., Peng, T.-H., Huang, W.-J., 2013. The marine inorganic carbon system along the Gulf of Mexico and Atlantic coasts of the United States: insights from a transregional coastal carbon study. *Limnol. Oceanogr.* 58, 325–342. <https://doi.org/10.4319/lo.2013.58.1.0325>.

White, J.R., DeLaune, R.D., Justic, D., Day, J.W., Pahl, J., Lane, R.R., Boynton, W.R., Twilley, R.R., 2019. Consequences of Mississippi River diversions on nutrient dynamics of coastal wetland soils and estuarine sediments: a review. *Estuar. Coast Shelf Sci.* 224, 209–216. <https://doi.org/10.1016/j.ecss.2019.04.027>.

Xue, L., Cai, W.-J., 2020. Total alkalinity minus dissolved inorganic carbon as a proxy for deciphering ocean acidification mechanisms. *Mar. Chem.* 222 <https://doi.org/10.1016/j.marchem.2020.103791>.

Yu, K., DeLaune, R.D., Boeckx, P., 2006. Direct measurement of denitrification activity in a Gulf coast freshwater marsh receiving diverted Mississippi River water. *Chemosphere* 65, 2449–2455. <https://doi.org/10.1016/j.chemosphere.2006.04.046>.